Electron-phonon scattering in Si and Ge: from bulk to nanodevices

D. Rideau[a], W. Zhang[b], Y. M. Niquet[c], C. Delerue[b], C. Tavernier[a], and H. Jaouen[a]
[a] STMicroelectronics, 850, rue J. Monnet, FR 38926 Crolles; denis.rideau@st.com.
[b] IEMN - Dept. ISEN, 59046 Lille Cedex, France.
[c] L_Sim, SP2M, UMR-E CEA/UJF-Grenoble 1, INAC, Grenoble, F-38054, France

***Abstract*—Using a $sp^3d^5s^*$ tight-binding model for the electrons and a valence force field model for the phonons, we investigate the electron-phonon scattering rates in Si and Ge. The bulk Si mobility calculated with this model ($\mu = 1400$ cm^2/V/s) and its temperature dependence agree well with experimental data. We are able to analyze the much lower values obtained in Si nanowires where both carriers and phonons are confined.**

I. Introduction

Silicon nanowires (SiNWs) have attracted significant interest as promising building blocks for nanotechnologies. They can be fabricated by bottom-up approaches [1] or by techniques compatible with standard complementary metal-oxide semiconductor (CMOS) process [2]–[4]. Recently, SiNWs with diameter d below 12 nm have been manufactured with excellent structural properties, which opens new opportunities for the design of nanoscale devices and for the exploration of quantum transport phenomena in low-dimensional systems. SiNWs can be used to build gate-all-around transistors in which short channel effects are reduced thanks to a better gate control, and transistors based on arrays of vertically stacked SiNWs with diameter close to 10 nm have been recently reported [5], [6]. In this context, it is essential to understand the effects of quantum confinement on the transport properties of small SiNWs, and to elucidate mobility-limiting mechanisms [7]–[17].

During the last three decades the intrinsic transport properties in strained nanodevices (such as the mobility and the saturation velocity) have been extensively studied using, e.g., full band Monte Carlo simulations. Considering that at room temperature, the transport properties of Si- and Ge-based devices strongly depend on the carrier-phonon interactions, it may come as a surprise that a full quantum treatment of this interaction (and in particular its variation with mechanical stress and with quantum confinement) is still incomplete. Most of the calculations available so far in Si and Ge rely on empirical isotropic deformation potentials (assuming either the overlap integral to be unity [18], [19] or adopting the Nordheim approximation [19]–[22]). Pseudo-potential-based studies taking into account the full anisotropy of the scattering rates have been performed in bulk Si by Kunikiyo *et al.* [23]. However, despite the significant progress achieved by these authors, the former calculations (as pointed out by Nguyen and Hofmann [21]) use an incorrect formulation of the atomic position in the unit cell. It ought to be noted that a recent first principle quantum-mechanical treatment with density functional theory (DFT) of the electron-phonon scattering rates in Si [24] highlighted noticeable discrepancies with previous semi-empirical results.

In this work, we investigate electron-phonon scattering in bulk Si, Ge, and in SiNWs with a fully atomistic semi-empirical approach. We use a recently developed $sp^3d^5s^*$ tight-binding (TB) model for the electronic structure [25] and a valence force field model for the phonons [26]. This tight-binding model reproduces the deformation potentials of Si and Ge in the whole first Brillouin zone and shall therefore be appropriate for the description of the electron-phonon interaction. We briefly review the computational details in the next section, then discuss the main results and conclusions in section III. We focus here on the low-field mobility as a metrics of the electron-phonon coupling strength and performances of the nanodevices.

II. Computational Methods

As testified by the increasing number of calculations, the atomistic TB method is well suited to the description of the electrical properties of nanodevices. Recently, several improvements have been introduced in the TB models to account for arbitrary strains [25], [27], [28]. It is, therefore, now possible to perform a rigorous atomistic calculation of the carrier-phonon interaction from bulk materials to, e.g., nanowires. The results presented here follow the methodology of Ref. [17], in which the electron-phonon interaction is expanded as a function of the derivatives of the Hamiltonian with respect to the atomic displacements. The phonons are computed with the valence force field model of Ref. [26]. All possible couplings between electron bands and phonon modes are taken into account in the calculations.

We consider a system subject to a homogeneous electric field $\mathbf{E} = E\mathbf{u}$, and split the distribution function $f_{n\mathbf{k}}$ of band n and wave vector $\mathbf{k}$ in two parts, $f_{n\mathbf{k}} \simeq f^0_{n\mathbf{k}} + eEg_{n\mathbf{k}}$, where f^0 is the equilibrium Fermi-Dirac distribution function, and $eEg_{n\mathbf{k}}$ is the first order variation of the distribution function. The $g_{n\mathbf{k}}$'s fulfill the equations:

$$\mathbf{u}\cdot\mathbf{v}_{n\mathbf{k}}\frac{df^0_{n\mathbf{k}}}{d\varepsilon} = \sum_m \int d\mathbf{k}'\rho(\mathbf{k}') \; g_{n\mathbf{k}}\left\{W(n\mathbf{k},m\mathbf{k}')[1-f^0_{m\mathbf{k}'}] + W(m\mathbf{k}',n\mathbf{k})f^0_{m\mathbf{k}'}\right\} - \; g_{m\mathbf{k}'}\left\{W(m\mathbf{k}',n\mathbf{k})[1-f^0_{n\mathbf{k}}] + W(n\mathbf{k},m\mathbf{k}')f^0_{n\mathbf{k}}\right\} \quad (1)$$

978-1-61284-418-3/11/$26.00 © 2011 IEEE

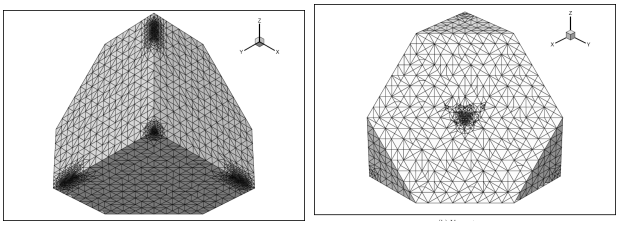

Fig. 1: The calculation of the electron-phonon scattering rate in bulk materials require a 3D integration of $W(n\mathbf{k}, m\mathbf{k}')$ over the full Brillouin Zone. This integration is performed on a dense mesh with 310 480 tetrahedra: (left) One eighth of the mesh showing dense regions near Δ valleys; (right) Same but showing another dense region near L valleys.

where $\mathbf{v}_{n\mathbf{k}}$ is the electronic group velocity, $W(n\mathbf{k}, m\mathbf{k}')$ is the scattering rate between bands $n\mathbf{k}$ and $m\mathbf{k}'$ computed with Fermi Golden rule [17], and $\rho(\mathbf{k})$ is the density of k-points in reciprocal space. The above linear system of equations couples all $g_{n\mathbf{k}}$'s together and can be very large. In bulk materials, the integration over $\mathbf{k}'$ is performed on a dense tetrahedral mesh (310 480 tetrahedra) with the Gilat-Raubenheimer method (see Fig. 1), and Eqs. (1) are solved iteratively until self-consistency is achieved ($4-5$ iterations). In nanowires, the integration is performed on a regular 1024 k-points mesh of the 1D Brillouin zone, and the above linear system of equations is directly inverted with LAPACK. Once the $g_{n\mathbf{k}}$ have been calculated, the mobility is given by:

$$\mu = -e\frac{\sum_n \int d\mathbf{k}\rho(\mathbf{k}) g_{n\mathbf{k}} \mathbf{u}\cdot\mathbf{v}_{n\mathbf{k}}}{\sum_n \int d\mathbf{k}\rho(\mathbf{k}) f^0_{n\mathbf{k}}}\,. \qquad (2)$$

III. Results and Discussion

The room-temperature mobilities computed in bulk Si with this methodology and 3 different $sp^3d^5s^*$ TB models [25], [27], [28] are reported in Table I. The model of Ref. [25], which has been designed to reproduce all deformation potentials of Si, yields bulk mobilities in excellent agreement with the experimental data ($\mu_{\text{exp}} = 1400$ cm^2/V/s). This agreement extends over (at least) the whole temperature range relevant for technological applications, as shown in Fig. 2. The mobility computed in bulk Germanium with the same model, $\mu = 4900$ cm^2/V/s, is, on the other hand, 25% larger than expected ($\mu_{\text{exp}} = 3900$ cm^2/V/s). It is however unclear at present whether this discrepancy results from the TB model itself (the deformation potentials of bulk Ge are not as well characterized as those of bulk Si), or from deficiencies of, e.g., the Fermi Golden rule. From now on, we focus on the results obtained with the TB model of Ref. [25].

Model	μ (cm^2/V/s)
Ref. [25]	1407
Ref. [27]	1770
Ref. [28]	2141

TABLE I: Room-temperature mobility computed at low carrier density in bulk Si with three different $sp^3d^5s^*$ TB models [25], [27], [28].

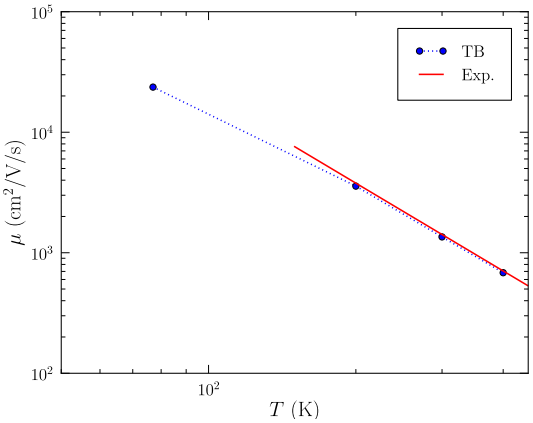

Fig. 2: The bulk mobility in silicon as a function of temperature T, computed with the TB model of Ref. [25], and compared with the experimental data $\mu = 1400(T/300)^{-2.42}$ for $T > 150$ K.

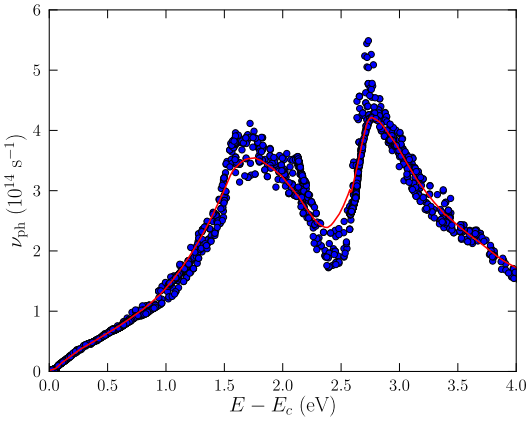

Fig. 3: The total scattering rate $\nu_{n\mathbf{k}} = \sum_{m\mathbf{k}'} W(n\mathbf{k}, m\mathbf{k}')$ in bulk Si as a function of the energy E of the incident electron $n\mathbf{k}$. The blue dots are individual $\nu_{n\mathbf{k}}$ points, showing the dispersion, and the solid red line is the average (weighted by the density of states at each individual point). E_c is the conduction band edge energy.

The total scattering rate $\nu_{n\mathbf{k}} = \sum_{m\mathbf{k}'} W(n\mathbf{k}, m\mathbf{k}')$ in bulk Si is plotted as a function of the energy E of the incident electron $n\mathbf{k}$ in Fig. 3. This figure shows the typical dispersion of the scattering rate from single $n\mathbf{k}$ points (individual blue dots) around the average value (solid red line).

The total scattering rate obtained with the TB model of Ref. [25] is compared with other semi-empirical and *ab initio* approaches in Figs. 4 (Si) and 5 (Ge). While all methods agree on the overall shape and magnitude of the electron-phonon scattering rates, there are significant discrepancies in the 0.3–1 eV range, which corresponds to high field transport in advanced nanodevices (see also Ref. [19] for a larger set of empirical results). In particular, the scattering rates in Si are significantly larger at high energy with the TB model of Ref. [25] than with other semi-empirical approaches. We note,

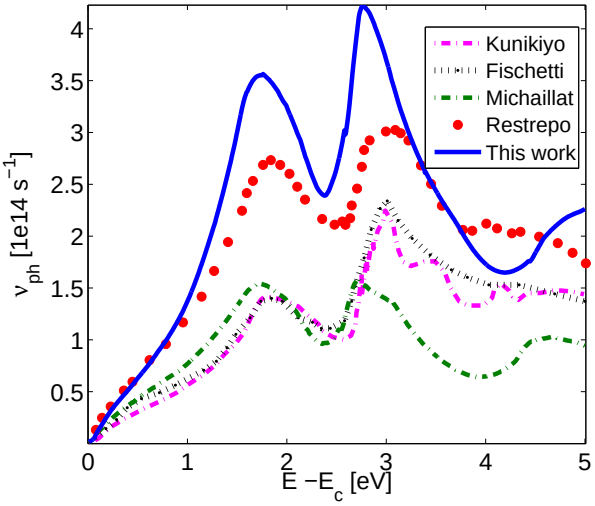

Fig. 4: The total scattering rate $\nu_{n\mathbf{k}} = \sum_{m\mathbf{k}'} W(n\mathbf{k}, m\mathbf{k}')$ in bulk Si as a function of the energy E of the incident electron $n\mathbf{k}$. The TB model of Ref. [25], the semi-empirical models of Refs. [20] and [22], and the *ab initio* density functional theory results of Ref. [24] are compared. E_c is the conduction band edge energy.

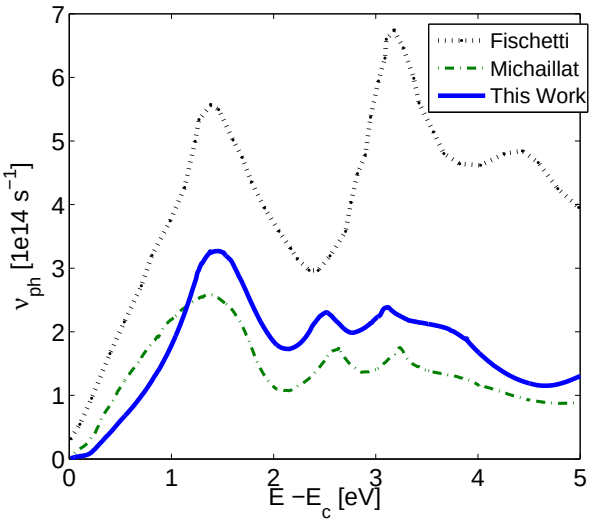

Fig. 5: The total scattering rate $\nu_{n\mathbf{k}} = \sum_{m\mathbf{k}'} W(n\mathbf{k}, m\mathbf{k}')$ in bulk Ge as a function of the energy E of the incident electron $n\mathbf{k}$. The TB model of Ref. [25], and the semi-empirical model of Refs. [20] and [22] are compared. E_c is the conduction band edge energy.

though, that this trend is corroborated by the recent *ab initio* density functional theory calculations of Ref. [24]. As for Ge, the TB scattering rates lie between the semi-empirical results of Refs. [20] and [22]. Ongoing calculations of the saturation velocity for the different models shall clarify the situation, but are beyond the scope of the present work.

We now discuss the case of free-standing (hydrogen passivated) silicon nanowires. The total scattering rate $\nu_{n\mathbf{k}} = \sum_{m\mathbf{k}'} W(n\mathbf{k}, m\mathbf{k}')$ in a 4 nm diameter $\langle 001 \rangle$ SiNW is plotted as a function of the energy of the incident electron in Fig. 7. At

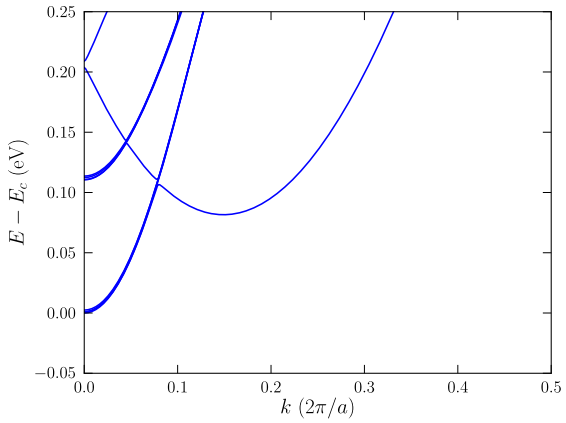

Fig. 6: Band structure of a 4 nm diameter $\langle 001 \rangle$ SiNW. E_c is the conduction band edge energy. The lowest-lying valleys at Γ are almost fourfold degenerate, while the higher-lying valleys off Γ are twofold degenerate.

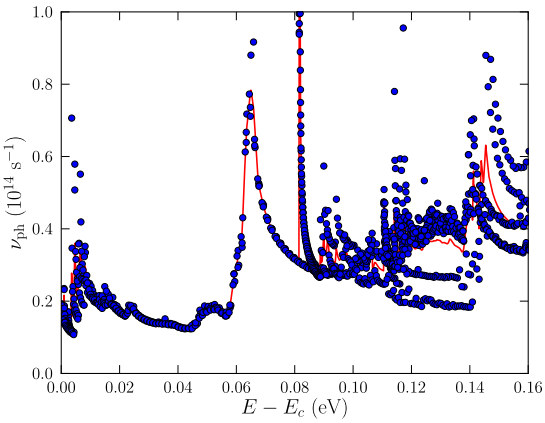

Fig. 7: The total scattering rate $\nu_{nk} = \sum_{mk'} W(nk, mk')$ in a 4 nm diameter $\langle 001 \rangle$ SiNW as a function of the energy E of the incident electron. The blue dots are individual ν_{nk} points, showing the dispersion, and the solid red line is the average (weighted by the density of states at each individual point). E_c is the conduction band edge energy. The first group of peaks is associated with the first (almost fourfold degenerate) subbands at Γ, and the second group of peaks around 70 meV to the higher-lying valleys off Γ (see Fig. 6).

variance with the bulk, the scattering rate exhibits a complex structure, with multiple Van Hove singularities typical of 1D systems. The first group of peaks in Fig. 7 is related to intraband acoustic scattering within the (almost) fourfold degenerate valley at Γ, while the second group around 70 meV is associated with the two higher lying valleys off Γ (see band structure in Fig. 6). There are multiple replicas of the main peaks characteristic of the phonon subband structure. The scattering rates are, on average, larger than in the bulk within the same energy range, suggesting an enhancement of the electron-phonon interaction in confined nanowires.

The TB, phonon-limited mobility in $\langle 001 \rangle$ SiNWs is plotted

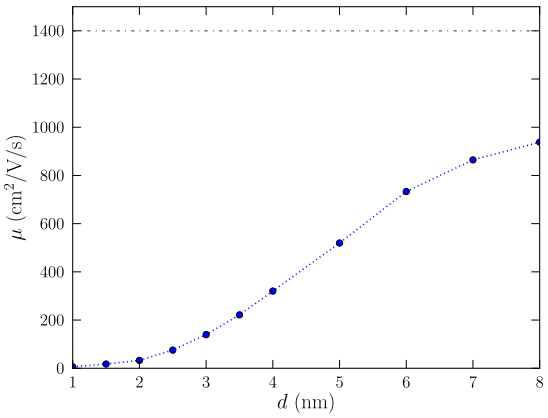

Fig. 8: The room-temperature TB mobility in $\langle 001 \rangle$ SiNWs as a function of nanowire diameter d. The horizontal dash-dotted line is the bulk limit. The carrier density is $n = 10^{18}$ cm^{-3}.

as a function of the nanowire diameter d in Fig. 8, in the 1–8 nm range. As expected from Fig. 7, the mobility is strongly hindered by the phonons in the smallest nanowires, and slowly increases with diameter. It is reduced by more than two-third in < 5 nm diameter nanowires, and still by $\simeq 20\%$ in 10 nm diameter nanowires. This shows that the benefits of quantum confinement (decrease of intersubband and intervalley scattering) do not overcome the strong enhancement of the electron-phonon interaction in small nanowires.

IV. Conclusions

We have discussed electron-phonon scattering in bulk Si and Ge and in Si nanowires within an atomistic framework. We have used a $sp^3d^5s^*$ tight-binding model for the electrons [25], designed to reproduce the deformation potentials of the bulk materials in the whole first Brillouin zone, and a valence force field model for the phonons [26]. All possible scatterings between electron bands and phonon modes have been taken into account. The TB mobility is in excellent agreement with experimental data in bulk Si, but overestimates the mobility by about 25% in bulk Ge. The total scattering rate is larger at high energy (high bias) in the TB description than in previous semi-empirical studies, but in close agreement with recent *ab initio* data obtained with density functional theory. This model, applied to SiNWs with diameters in the 1–8 nm range, shows that the electron-phonon interaction is a major source of scattering in ultimate nanodevices. The low-field mobilities can indeed be reduced by more than 70% in < 5 nm diameter $\langle 001 \rangle$ Si nanowires, and by $\simeq 20\%$ in 10 nm ones.

Acknowledgment

This work was supported by the French National Research Agency (ANR) project "Quasanova". A part of the calculations was done at CCRT.

References

[1] V. Schmidt, J. V. Wittemann, and U. Gösele, Chem. Rev. **110**, 361 (2010).
[2] G. Pei, J. Kedsierski, P. Oldiges, M. Ieong, and E. C. C. Kan, IEEE Trans. Electron Devices **49**, 1411 (2002).
[3] P. Colinge, Solid-State Electron. **48**, 897 (2004).
[4] S. D. Suk, S.-Y. Lee, S.-M. Kim, E.-J. Yoon, M.-S. Kim, M. Li, C. W. Oh, K. H. Yeo, S. H. Kim, D.-S. Shin, K.-H. Lee, H. S. Park, J. N. Han, C. J. Park, J.-B. Park, D.-W. Kim, D. Park, and B.-I. Ryu, IEDM Tech. Digest 2005, 717 (2005).
[5] C. Dupré, A. Hubert, S. Bécu, M. Jublot, V. Maffini-Alvaro, C. Vizioz, F. Aussenac, C. Arvet, S. Barnola, J.-M. Hartmann, G. Garnier, F. Allain, J.-P. Colonna, M. Rivoire, L. Baud, S. Pauliac, V. Loup, P. Rivallin, B. Guillaumot, G. Ghibaudo, O. Faynot, T. Ernst, and S. Deleonibus, IEDM Tech. Digest 2008, 749 (2008).
[6] R. M. Y. Ng, T. Wang, F. Liu, X. Zuo, J. He, and M. Chan, IEEE Electron Device Lett. **30**, 520 (2009).
[7] V. A. Fonoberov and A. A. Balandin, Nano Lett. **6**, 2442 (2006).
[8] M. V. Fernández-Serra, Ch. Adessi, and X. Blase, Phys. Rev. Lett. **96**, 166805 (2006).
[9] T. Markussen, R. Rurali, A.-P. Jauho, and M. Brandbyge, Phys. Rev. Lett. **99**, 076803 (2007).
[10] M. P. Persson, A. Lherbier, Y. M. Niquet, F. Triozon, and S. Roche, Nano Letters **8**, 4146 (2008).
[11] R. Rurali, T. Markussen, M. Brandbyge, and A.-P. Jauho, Nano Lett. **8**, 2825 (2008).
[12] E. B. Ramayya, D. Vasileska, S.M. Goodnick, I. Knezevic, J. Appl. Phys. **104**, 063711 (2008).
[13] M. Luisier and G. Klimeck, Phys. Rev. B **80**, 155430 (2009).
[14] F. Murphy-Armando, G. Fagas, and J. C. Greer, Nano Lett. **10**, 869 (2010).
[15] M. Bescond, M. Lannoo, L. Raymond, and F. Michelini, J. Appl. Phys. **107**, 093703 (2010).
[16] M. P. Persson, H. Mera, Y. M. Niquet, C. Delerue, and M. Diarra, Phys. Rev. B **82**, 115318 (2010).
[17] W. Zhang, C. Delerue, Y. M. Niquet, G. Allan, and E. Wang, Phys. Rev. B **82**, 115319 (2010).
[18] E. Pop *et al.*, J. Appl. Phys. **96**, 4998 (2004).
[19] A. Abramo *et al.*, IEEE. Trans. Electron Devices **41**, 1646 (1994).
[20] M. V. Fichetti and S. Laux, J. Appl. Phys. **80**, 2234 (1996); IEEE Trans. Elec. Device **38**, 634 (1991).
[21] P. H. Nguyen *et al.*, J. Appl. Phys. **92**, 5359 (2002); P. H. Nguyen *et al.*, J. Appl. Phys. **94**, 375 (2003).
[22] M. Michaillat *et al.*, J. of Phys: Conference Series **193**, 1 (2009); M. Michaillat *et al.*, Thin Solid Films **518**, 2437 (2010).
[23] T. Kunikiyo *et al.*, J. Appl. Phys. **75**, 297 (1994).
[24] O. D. Restrepo *et al.*, J. Appl. Phys. **94**, 212103 (2009).
[25] Y. M. Niquet, D. Rideau, C. Tavernier, H. Jaouen, and X. Blase, Phys. Rev. B **79**, 245201 (2009).
[26] D. Vanderbilt, S. H. Taole, and S. Narasimhan, Phys. Rev. B **40**, 5657 (1989).
[27] T. B. Boykin, N. Kharche, and G. Klimeck, Phys. Rev. B **76**, 035310 (2007).
[28] J.-M. Jancu, R. Scholz, F. Beltram, and F. Bassani, Phys. Rev. B **57**, 6493 (1998).